FORM TI-12
8/94

WAPD-T-3145

CONF-970824--13

ONE-GROUP INTERFACIAL AREA TRANSPORT IN VERTICAL AIR-WATER BUBBLY FLOW

Q. Wu, S. Kim and M. Ishii
Purdue University

S. G. Beus
Westinghouse Electric Corporation

DE-AC11-93PN38195

BETTIS ATOMIC POWER LABORATORY WEST MIFFLIN, PENNSYLVANIA 15122-0079

Operated for the U.S. Department of Energy
by WESTINGHOUSE ELECTRIC CORPORATION

DISCLAIMER

ONE-GROUP INTERFACIAL AREA TRANSPORT IN VERTICAL AIR-WATER BUBBLY FLOW

Q. Wu, S. Kim and M. Ishii
Thermal Hydraulics and Reactor Safety Laboratory
Purdue University
West Lafayette, IN 47907, U.S.A.
(765) 494-5759

S.G. Beus
Bettis Atomic Power Lab.
Westinghouse Electric Corporation
Box 79, West Mifflin, PA 15122, USA.
(412) 476-6430

ABSTRACT

In the two-fluid model for two-phase flows, interfacial area concentration is one of the most important closure relations that should be obtained from careful mechanistic modeling. The objective of this study is to develop a one-group interfacial area transport equation together with the modeling of the source and sink terms due to bubble breakage and coalescence. For bubble coalescence, two mechanisms are considered to be dominant in vertical two-phase bubbly flow. These are the random collisions between bubbles due to turbulence in the flow field, and the wake entrainment process due to the relative motion of the bubbles in the wake region of a seeding bubble. For bubble breakup, the impact of turbulent eddies is considered. These phenomena are modeled individually, resulting in a one-group interfacial area concentration transport equation with certain parameters to be determined from experimental data. Compared to the measured axial distribution of the interfacial area concentration under various flow conditions, these parameters are obtained for the reduced one-group, one-dimensional transport equation. The results indicate that the proposed models for bubble breakup and coalescence are appropriate.

I. INTRODUCTION

In the analysis of two-phase flow, the formulation using a two-fluid model is considered the most accurate model. With proper averaging in this model, the two phases are considered separately in terms of two sets of conservation equations that govern the balance of mass, momentum and energy in each phase (Vernier and Delhaye, 1965 [1]; Kocamustafaogullari, 1971 [2]; M. Ishii, 1975 [3]; Boure, 1978 [4]). However, the averaged macroscopic fields of the two phases are not independent of each other, and there are certain phase interaction terms in the field equations to characterize the interfacial transfers of mass, momentum and energy. These terms contain a parameter that specifies the geometric capability of the interfacial transfers, i.e., the interfacial area concentration (or density), defined as the total surface area of the dispersed fluid particles per unit mixture volume (Ishii and Mishima, 1980 [5]). Therefore, a closure relation of the interfacial area concentration is indispensable in the two-fluid model for detailed treatment of the phase interactions. In other words, a mathematical description of this area concentration should be developed in terms of the field variables of the two-phase flow.

Since the interfacial area concentration changes with the variation of the particle number density due to coalescence and breakage, analogous to Boltzman's transport equation, a Population Balance Approach (PBA) was recently proposed by Reyes (1989 [6]) to develop a particle number density transport equation for chemically non-reacting, dispersed spherical fluid particles. A similar method was employed in combustion theory, known as the spray-equation (Williams, 1965 [7]). For the purpose of interfacial area transport, Kocamustafaogullari and Ishii (1995 [8]) generalized Reyes' model, leading to the following equation:

$$\frac{\partial f(\bar{x}, \mathcal{V}, t)}{\partial t} + \nabla \cdot \left(f(\bar{x}, \mathcal{V}, t) \mathbf{v}_p \right) = \sum_j s_j(\bar{x}, \mathcal{V}, t) + s_{ph}(\bar{x}, \mathcal{V}, t) \quad (1)$$

where $f(\bar{x}, \mathcal{V}, t)$ is the particle density distribution function, which is assumed to be continuous and specifies the probable number of fluid particles at a given time t, in

the spatial range of $d\bar{x}$ about a position $\bar{x}$, with particle volumes between $\mathcal{V}$ and $\mathcal{V}+d\mathcal{V}$. Moreover, $v_p(\bar{x}, \mathcal{V}, t)$ denotes the local time-averaged velocity of the particles with volume between $\mathcal{V}$ and $\mathcal{V}+d\mathcal{V}$, and $s_{ph}(\bar{x}, \mathcal{V}, t)$ refers to the fluid particle sink or source rate due to phase change. If the phase change only causes fluid particle shrinkage or expansion, s_{ph} can be expressed in the form of $-\partial / \partial t(f\, d\mathcal{V} / dt)$, which Shraiber (1996 [9]) thought it should be presented on left hand of Eq. (1). However, for the case of homogeneous nucleation boiling or condensation in a subcooled boiling flow, s_{ph} should also include the population change rate of fluid particles with specific volumes. Detailed treatment of the phase change term may follow the approach suggested by Kocamustafaogullari and Ishii (1983 [10]), whereas the wall nucleation rate must be specified as a boundary condition.

The interaction terms in Eq. (1), $s_j(\bar{x}, \mathcal{V}, t)$, represent the net rate of change in the particle number density distribution function caused by particle breakup and coalescence processes. Some phenomenological models for these terms were summarized by Prince and Blanch (1990 [11]) and Lafi and Reyes (1991 [12]). These models presented the detailed insight of the mechanisms for coalescence and breakage phenomena. However, due to the dependence on the fluid particle volume, many adjustable parameters and assumptions were imposed, which may be far beyond the ability of justification with the existing experimental data. For most two-phase flow studies, where the primary focus is on the average fluid particle behavior, the detailed volume dependent particle number density transport equation would be too tedious and complicated for the field equations in practical applications. From this point of view, the present study starts from the integral form of particle number density transport equation, i.e.,

$$\frac{\partial n(\bar{x}, t)}{\partial t} + \nabla \cdot \left(\mathbf{v}_{pm}(\bar{x}, t)\, n(\bar{x}, t) \right) = \sum_j S_{nj}(\bar{x}, t) + S_{nph}(\bar{x}, t) \quad , \qquad (2)$$

where $n(\bar{x}, t)$ is the total number of particles of all sizes per unit mixture volume, and $\mathbf{v}_{pm}(\bar{x}, t)$ is the average local particle velocity weighted by the particle number. This velocity is identical to the time-averaged bubble velocity weighted by the gas void fraction, i.e., $\bar{\mathbf{v}}_g$ in the time-averaged two-fluid model (Ishii, 1975 [3]), if the statistical sample size is sufficiently large. The major efforts here will focus on the integral source and sink terms caused by binary coalescence and breakage of single size particles. Furthermore, because of the differences in inertia and buoyancy forces between liquid droplets and gas bubbles, unified models for the source and sink terms are unlikely at least for the adjustable coefficients. Therefore, the models developed in this study will be limited only to the two-phase flow system with the dispersed phase as gas bubbles.

A general approach treats the bubbles in two groups: the spherical/distorted bubble group and the cap/slug bubble group (Ishii and Kojasoy, 1993 [13]). Because of the differences in bubble shapes and mobility of the two groups, two bubble number density transport equations are required that involve the inner and inter group interactions as shown in Fig. 1. The mechanisms of these interactions can be summarized in five categories. They are the coalescence due to random collisions driven by turbulence, the coalescence due to wake entrainment, the breakage upon the impact of turbulent eddies, the shearing-off of small bubbles from the skirt of cap bubbles, and the breakage of large cap bubbles due to flow instability on the bubble surface. Some other mechanisms such as the laminar shearing induced coalescence (Friedlander, 1977 [14]) and the breakage due to velocity gradient (Taylor, 1934 [15]) are excluded.

The laminar shearing induced collision occurs at high gas flow rate. Bubbles rise preferentially through the center of a pipe. A gross circulation pattern is thus formed with a net upward velocity in the column center and a down flow in the outer annular region near the wall. This flow pattern gives rise to a radial velocity distribution, and the bubbles in the center zone would overtake the bubbles of same size in the outer zone. However, the direct result of the flow pattern should be the mean flow parameters and bubble number density distributions. This phenomenon is governed by the field equations especially including the lateral force such as the lift force proposed by Drew and Lahey (1987 [16]). Under such a condition, the coalescence should also be directly induced by localized random collision rate or wake-entrainment rate. Therefore, the laminar shearing induced collision is eliminated here as an independent mechanism. On the other hand, the bubble breakup due to velocity gradient, according to Clift et al. (1978 [17]), occurs in viscous flow with large velocity gradient. For the case of low viscosity flow like in air-water or steam-water system, the velocity profile is relatively flat. Moreover, the high mobility of gas bubbles allows bubbles to be redistributed by shear force before disintegration. Therefore, this mechanism is also excluded.

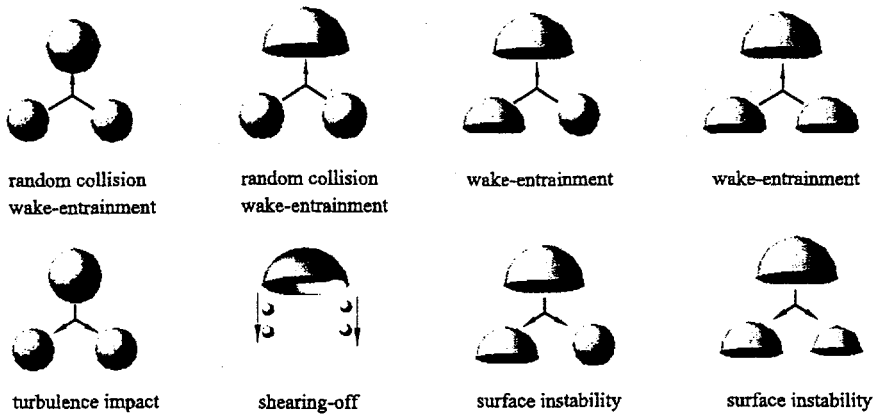

Fig. 1 Mechanisms of bubble coalescence and break-up in two-group model

In practice, when the void fraction of a two-phase bubbly flow is small, no cup or slug bubble exists. The two-group transport equations is then reduced to one group, and the interactions between the two groups can be omitted. As the first step of the general approach, the focus of this study is on the first group transport equation for bubbly flow without the occurrence of cap or slug bubbles. In section two, three models are developed for bubble coalescence and breakage, including the bubble coalescence due to random collisions driven by turbulence, bubble coalescence due to wake entrainment, and bubble breakage upon the impact of turbulent eddies. With these models, the one-group interfacial area transport equation is obtained in section three, whereas the adjustable parameters are evaluated in section four with the existing experimental data obtained from vertical two-phase bubbly flow (Kashyap et al, 1994 [18]). This approach provides a solid foundation for the latter phase investigation of the two-group transport equations to obtain the general closure relation of interfacial area concentration for the two-fluid model.

II. MODELING OF BUBBLE COALESCENCE AND BREAKAGE

For dispersed bubbly flow without phase change, only three mechanisms responsible for bubble coalescence and breakage are considered in the one-group bubble number density transport equation:

$$\frac{\partial n(\vec{x}, t)}{\partial t} + \nabla \cdot \left(\vec{\mathbf{v}}_g(\vec{x}, t)\, n(\vec{x}, t) \right) = S_{n,RC}(\vec{x}, t) + S_{n,WE}(\vec{x}, t) + S_{n,TI}(\vec{x}, t) \qquad (3)$$

The terms on the right hand side of Eq.(3) are the bubble number source and sink rate per unit mixture volume with a subscript "n" standing for net bubble number density change, "*RC*" for random collision due to turbulence in the continuous medium, "*WE*" for wake-entrainment caused by the relative motion between the bubbles in the wake region and the seeding bubble, and "*TI*" for turbulent eddies that impact the bubbles resulting in bubble breakage. The disunion of the transport equation from phase change effects and the existence of cap/slug bubbles not only greatly simplifies the investigation, but also enables effective justifications of the presented source and sink terms by comparing the model with experimental data. Moreover, the one-group transport equation with uniform bubble size matches the two-fluid model, which focuses on the average fluid particle behavior without considering the detailed bubble volume dependence. Here, the average bubble size is characterized by the bubble Sauter mean diameter, D:

$$D = \frac{6 \int_{\mathcal{V}} \mathcal{V} f(\vec{x}, \mathcal{V}, t)\, d\mathcal{V}}{\int_{\mathcal{V}} a_{\mathcal{V}} f(\vec{x}, \mathcal{V}, t)\, d\mathcal{V}} = \frac{6\alpha(\vec{x}, t)}{a_i(\vec{x}, t)}, \qquad (4)$$

with $a_{\mathcal{V}}$ as the surface area of a bubble with volume $\mathcal{V}$, α as the local time-averaged gas void fraction, and a_i representing the local time-averaged interfacial area concentration. In this section, the source and sink terms in Eq. (3) are modeled individually by assuming binary interactions between spherical bubbles.

A. Random Collision Induced Bubble Coalescence

In bubbly flow, one of the mechanisms that drives bubbles together is the turbulence in the continuous medium. To model the bubble coalescence rate induced by this mechanism, the bubble random collision rate is of primary importance. These collisions are postulated to occur only between neighboring bubbles, because long range interactions are driven by large eddies that

transport groups of bubbles without leading to significant relative motion [11, 19]. Between the two neighboring spherical bubbles of the same size as shown in Fig. 2, the time interval for one collision is given by:

$$\Delta t = \frac{\bar{L}}{u_t}, \tag{5}$$

where u_t is the root-mean-square approaching velocity, and $\bar{L}$ denotes the mean distance between the two bubbles, i.e.,

$$\bar{L} \approx De - \delta D. \tag{6}$$

Here, De is the effective diameter of the mixture volume that contains one bubble. In terms of the local time-averaged void fraction and bubble Sauter mean diameter D, De is given by:

$$De \propto \frac{D}{\alpha^{1/3}}. \tag{7}$$

Since the bubble traveling length for one collision varies from De to (De-D), a factor δ is introduced into Eq. (6) to feature the average effect. By substituting Eq. (7) into Eq. (6), the average traveling length is given by:

$$\bar{L} \approx De - \delta D \propto \left(\frac{D}{\alpha^{1/3}} - \delta_1 D\right) = \frac{D}{\alpha^{1/3}}\left(1 - \delta_1 \alpha^{1/3}\right), \tag{8}$$

where δ_1 is a collective parameter considering the proportional sign between De and $D/\alpha^{1/3}$. At small void fraction, the modifying factor, δ_1, plays a minor role due to the fact that De is much larger than D. However, it is important if the traveling length is comparable to the bubble size. When the void fraction approaches the dense packing limit ($\alpha = \alpha_{max}$), the mean traveling length should be zero, which leads to δ_1 equal to $\alpha_{max}^{-1/3}$. Using this asymptotic value as the approximation of δ_1, the mean traveling length is reduced to:

$$\bar{L} \propto \frac{D}{\alpha^{1/3}}\left[1 - \left(\frac{\alpha}{\alpha_{max}}\right)^{1/3}\right]. \tag{9}$$

Accordingly, for the two bubbles moving toward each other, the collision frequency is given by:

$$r_{RC} = \frac{1}{\Delta t} \propto \frac{u_t}{D}\alpha^{1/3}\left[\frac{\alpha_{max}^{1/3}}{\alpha_{max}^{1/3} - \alpha^{1/3}}\right]. \tag{10}$$

Since the bubbles do not always move toward each other, however, a probability, P_C, for a bubble to move toward a neighboring bubble is introduced to modify the collision rate. By assuming a hexagonal close-packed structure as shown in Fig. 3, if the neighborhood bubbles are fixed in the lattice structure, this probability is given by:

$$P_c \sim \frac{D^2}{De^2} = \alpha^{2/3}, \quad \alpha < \alpha_c, \tag{11}$$

$$P_c = 1, \quad \alpha > \alpha_c, \tag{12}$$

where α_c is the critical void fraction when the center bubble can barely pass through the largest free space among the neighborhood bubbles. In reality, the neighboring bubbles are in constant motions, and thus the critical void fraction can be very high, close to the dense packing limit. From this point of view, an approximation of the probability is

$$P_c \sim \left(\frac{\alpha}{\alpha_{max}}\right)^{2/3}. \tag{13}$$

Multiplying (8) by P_c, the collision rate for a two-phase mixture with bubble number density n is obtained as:

$$R_{RC} \approx \frac{u_t}{\bar{L}} n P_c \propto n u_t \frac{\alpha}{D}\left[\frac{1}{\alpha_{max}^{1/3}(\alpha_{max}^{1/3} - \alpha^{1/3})}\right] \propto n^2 u_t D^2 \left[\frac{1}{\alpha_{max}^{1/3}(\alpha_{max}^{1/3} - \alpha^{1/3})}\right]. \tag{14}$$

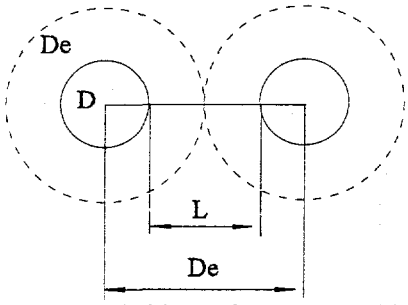

Fig. 2 Geometric definitions of two approaching bubbles

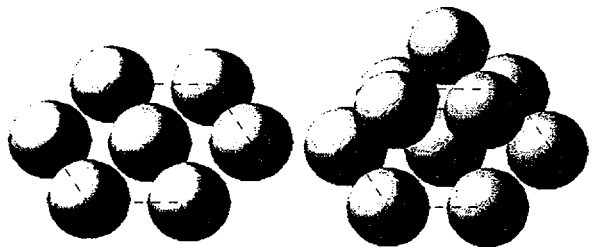

Fig. 3 Illustration of hexagonal closed packing structure

The functional dependence of the collision rate in Eq. (14) is similar to what Coulaloglou and Tavlarides [19] proposed in 1977 for a liquid-liquid droplet flow system, analogous to the particle collision model in an ideal gas. The difference is that the present model contains an extra term in the bracket, which covers the situation when the mean free path of bubbles is comparable to the bubble size. However, the model in the present form is still incomplete because no matter how far away the neighborhood bubble is located, the collision would occur as long as there is a finite approaching velocity. Actually, when the mean distance between the neighboring bubble is very large, no collision should be counted because the range of the relative motion between the neighboring bubbles is limited by the eddy size comparable to the bubble size. To consider this effect, a modification factor is introduced to Eq. (12), i.e.,

$$\left[1-\exp\left(-C\frac{L_t}{\bar{L}}\right)\right], \tag{15}$$

where L_t is the average size of the eddies that drive the neighboring bubbles. This effective eddy size is assumed to be of the same order of the mean bubble size, because smaller eddies do not provide considerable bulk motion to a bubble, while larger eddies transport groups of bubbles without leading to significant relative motion. Therefore, the bubble collision rate is modified to:

$$R_{RC} \sim \left(u_t n^2 D^2\right)\left[\frac{1}{\alpha_{\max}^{1/3}\left(\alpha_{\max}^{1/3}-\alpha^{1/3}\right)}\right]\left[1-\exp\left(-C\frac{\alpha_{\max}^{1/3}\alpha^{1/3}}{\alpha_{\max}^{1/3}-\alpha^{1/3}}\right)\right] \tag{16}$$

For each collision, coalescence may not occur and thus a collision efficiency was suggested by many investigators. A detailed review of the modeling efforts was given by Lafi and Reyes (1991 [12]). In general, the collision efficiency is defined as:

$$\eta_c \sim \exp(-\gamma), \tag{17}$$

where γ is determined by the mechanism of bubble coalescence upon each collision. The most popular model for collision efficiency is the film thinning model [20]. In this model γ is assumed to be the ratio of the average coalescence time to the average contact time. The bubble contact time refers to the time required for a bubble to travel a characteristic length driven by turbulence, while the coalescence time is defined as the time required for the liquid film thickness between the colliding particles to decrease from its initial thickness, h_0, to a critical thickness, h_c, which specifies the film thickness at the instant of rupture. Prince and Blanch [11] employed a film thinning model developed by Oolman and Blanch (1986 [20]), and provided a simplified expression for γ:

$$\gamma \sim \left(\frac{Du_t^2\rho_f}{\sigma}\right)^{1/2}\ln\left(\frac{h_0}{h_c}\right) = We_D^{1/2}\ln\left(\frac{h_0}{h_c}\right) \tag{18}$$

Since the critical film thickness and the initial film thickness depend on the fluid properties, γ is proportional to the square root of the Weber number. A physical explanation given by Kirkpatrick and Lockett (1974 [21]) is that when the bubbles approach faster, they intend to bounce back without coalescence due to the limitation of the film drainage rate governed by surface tension. However, flow visualization of Stewart (1995 [22]) shows that the bubble coalescence seems to be a random process. After collision, the bubbles always bounce away unless a "key" position is assumed, with one slightly ahead of the other. Once in the key position, the bubbles "dance" together, some times for several wobble cycles before coalescing or drifting away. This observation is not supportive to the film-thinning model that requires only the bubble motion upon collision slower than the drainage process regardless the relative position of the bubbles after collision. According to Steward, even when a key position is achieved, the bubbles may not necessarily coalesce, which also cannot be explained by the model. Mathematically, the proposed efficiency implies that the coalescence rate decreases exponentially with respect to the turbulent fluctuating velocity, which is much stronger than the linear dependence of the collision rate, resulting in an overall decreasing trend of the coalescence rate as the turbulent fluctuation increases. This caused serious trouble when the model was applied to experimental data following the procedure specified later in section 4. Tremendous discrepancies were obtained at different liquid flow conditions. For these reasons, a constant coalescence efficiency is assumed in the present model to depict the randomness of coalescence phenomena after each collision. Further studies on the coalescence efficiency is needed. Finally, the bubble coalescence rate due to random collisions caused by turbulent fluctuation is given by:

$$R_{RC} = \left[\frac{C_{RC}\left(u_t n^2 D^2\right)}{\alpha_{\max}^{1/3}\left(\alpha_{\max}^{1/3}-\alpha^{1/3}\right)}\right]\left[1-\exp\left(-C\frac{\alpha_{\max}^{1/3}\alpha^{1/3}}{\alpha_{\max}^{1/3}-\alpha^{1/3}}\right)\right]. \tag{19}$$

The coefficient C_{RC} and C are adjustable parameters, which depend on the fluid properties and should be obtained from experiments. The remaining unknowns are the maximum void fraction and the mean bubble fluctuating velocity. By definition, $\alpha_{\max}$ is the dense packing limit of void fraction when the coalescence rate approaches infinity. The mathematical expression of this value for spherical bubbles can be rigorously derived from the hexagonal close-packed structure, which leads $\alpha_{\max}$ equal to 0.65. However, the distortion of bubbles at

high liquid velocity may disobey the spherical bubble hypothesis and the bubble size distribution in reality may violate the uniform bubble size assumption, resulting in a higher dense packing limit. This case comes from the lower section of a vertical concurrent loop in slug flow regime, where dispersed bubbles exist and rapidly develop into gas slugs along the flow path due to significant bubble coalescence. Therefore, a rational choice of α_{max} should be at the transition point of slug flow to annular flow, i.e., α_{max} equal to approximately 0.8 (Wallis, 1969 [23]). This choice also leaves room for the one-group model to be applied with the second group transport equation at high void fraction conditions, where the assumption of dispersed bubbly flow is improper.

According to Ishii and Kojasoy (1993 [24]), the mean bubble fluctuating velocity, u_t in Eq. (17), is proportional to the root-mean-square liquid fluctuating velocity difference between two points of length scale D, which is given by (Batchelor, 1951 [25]):

$$u_t \sim \varepsilon^{1/3} D^{1/3} \tag{20}$$

where ε is the energy dissipation rate per unit mass of the continuous medium. In a complete two-fluid model, ε comes from its constitutive relation. The advanced approach for bubbly flow is the two-phase κ–ε model (Lee et al., 1989 [26]; Kataoka and Serizawa, 1991 [27]; Bertodano et al., 1994 [28]).

B. Wake-Entrainment Induced Bubble Coalescence

When bubbles enter the wake region of a leading bubble, they will accelerate and may collide with the preceding one (Nevers and Wu, 1971 [29]; Otake et al., 1977 [30]; Bilicki and Kestin, 1987 [31]; Stewart, 1995 [22]; Katz and Meneveau, 1996 [32]). For spherical bubbles, since the external flow is indistinguishable from that around a solid sphere at the same Reynolds number [17], the wake structure of a leading bubble can be analogous to that around a solid sphere. For an air bubble with attached wake region in water medium ($Re_D > 20$), the effective wake volume, in which the following bubbles may collide with the leading one, is defined as the projected area of the leading bubble multiplied by the effective length as illustrated in Fig. 4:

$$\mathcal{V}_w \approx \frac{1}{4}\pi D^2 \left(L_w - D/2\right) \tag{21}$$

The number of bubbles inside the effective volume is given by

$$N_w = \mathcal{V}_w n \approx \frac{1}{4}\pi D^2 (L_w - D/2) n . \tag{22}$$

Assuming the average time interval for a bubble in the wake region to catch up with the preceding bubble is ΔT, the collision rate per unit mixture volume is thus obtained:

$$\begin{aligned} R_{WE} &\propto \frac{1}{2} n \frac{N_w}{\Delta T} \\ &\approx \frac{1}{8}\pi D^2 n^2 \left(\frac{L_w - D/2}{\Delta T}\right) \approx \frac{1}{8}\pi D^2 n^2 \bar{u}_{rw} \end{aligned}, \tag{23}$$

where $\bar{u}_{rw}$ is the average relative velocity between the leading bubble and the bubble in the wake region. If the transient for a bubble to reach its terminal velocity is assumed much shorter than the collision process, the average relative velocity, $\bar{u}_{rw}$, can be expressed in terms of the relative velocities of the continuous medium inside and outside the wake region:

$$\bar{u}_{rw} \approx \left(\overline{V_f(z) - V_{f0}}\right), \tag{24}$$

with $V_f(z)$ as the local liquid velocity at the center line, z as the distance measured from the center of the leading bubble as shown in Fig. 4, and V_{f0} as the ambient liquid velocity. For a turbulent wake, which satisfies most of the practical bubbly flow regime, the wake velocity on the center line roughly satisfies (White, 1991 [32]):

$$V_f(z) - V_{f0} = u_r(D)\left(\frac{D/2}{z}\right)^{2/3} . \tag{25}$$

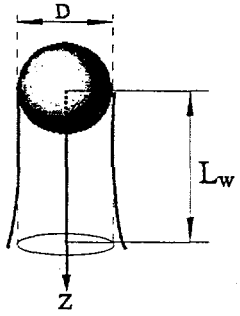

Fig. 4 Illustration of the wake of a leading bubble

Here, $u_r(D)$ is the terminal velocity of a bubble of diameter D. By integrating Eq. (25) over the effective wake length, (L_W - D/2), the average relative velocity in the wake region is given by:

$$\begin{aligned} \bar{u}_{rw} &\approx u_r(D)\left(\frac{3D/2}{L_w - D/2}\right)\left[\left(\frac{L_w}{D/2}\right)^{1/3} - 1\right] \\ &= u_r(D) F\left(\frac{D}{L_w}\right) \end{aligned} \tag{26}$$

The exact form of $F(D/L_W)$ is not important since the effective bubble wake region may not be fully established. According to Tsuchiya et al. (1989 [33]), the wake length is roughly 5 to 7 times the bubble diameter in air-water system, and thus D/L_W as well as $F(D/L_W)$ are treated as constants depending on the fluid properties. As long as their values obtained from experimental data fall into the range for D/L_W = 5~7, the mechanism should be acceptable. Substituting Eq. (26) into Eq. (23) yields the following simple expression of the bubble collision rate per unit mixture volume due to the wake-entrainment mechanism:

$$R_{WE} \propto F(\frac{D}{L_w})\frac{1}{4}D^2\frac{n^2}{2}u_r(D) \qquad (27)$$

The final form of the bubble coalescence rate for wake-entrainment is then given by

$$R_{WE} = C_{WE}D^2u_r(D)n^2 \ , \qquad (28)$$

where C_{WE} is an adjustable constant mainly determined by the ratio of the effective wake length to the bubble size. A proper choice for C_{WE} should yield an effective wake length roughly 5 to 7 from Eqs. (26) and (27). The bubble terminal velocity, u_r, is a function of the bubble diameter and local time-averaged void fraction. Based on the balance between the buoyancy force and drag force in a two-phase bubbly flow, Ishii and Chawla (1979 [34]) applied a drag-similarity criterion with the mixture-viscosity concept to obtain the following expression for the relative velocity:

$$u_r = \left(\frac{Dg}{3C_D}\frac{\Delta\rho}{\rho_f}\right)^{1/2}, \qquad (29)$$

with $$C_D = 24\frac{\left(1+0.1\,\mathrm{Re}_D^{0.75}\right)}{\mathrm{Re}_D},$$

and $$\mathrm{Re}_D \equiv \frac{\rho_f u_r D}{\mu_f}(1-\alpha). \qquad (30)$$

C. Bubble Breakup due to Turbulent Impact

For binary bubble breakup, the impact force comes from the inertia force, F_t, of the turbulent eddies in the continuous medium, while the holding force is the surface tension force, F_σ. To drive the daughter bubbles apart with a characteristic length of D, a simple momentum balance approach gives the following relation:

$$\frac{\rho_f D^3 D}{\Delta T^2} \propto F_t - F_\sigma, \qquad (31)$$

with ΔT as the average breaking time. Here, the inertia of the bubble is dominated by the virtual mass because of the large density ratio between liquid and gas. Rearranging Eq. (31) leads to the following average breakup time:

$$\Delta T \propto \frac{D}{u_t}\left(1-\frac{\mathrm{We}_{cr}}{\mathrm{We}}\right)^{-1/2}, \mathrm{We} = \frac{\rho_f u_t^2 D}{\sigma} > \mathrm{We}_{cr}. \qquad (32)$$

The velocity, u_t as defined in Eq. (20), is assumed to be the root-mean-square velocity difference between two points of length D, which implies that only the eddies having a size equivalent to the bubble size can break up the bubble. We_{cr} is a collective constant, designated as a critical Weber number. The reported value of We_{cr} for bubble breakup varies in a wide range due to the resonance excitation of the turbulent fluctuation (Sevik and Park, 1973 [35]). In an air-water system, Prince and Blanch [11] suggested that We_{cr} equals 2.3. From the defined bubble breakup time, if the bubble number density is n, the bubble breakup rate per unit mixture volume should be:

$$R_{TI} \propto n\frac{1}{\Delta T} = n\frac{u_t}{D}\left(1-\frac{\mathrm{We}_{cr}}{\mathrm{We}}\right)^{1/2}, \mathrm{We} > \mathrm{We}_{cr}. \qquad (33)$$

In a homogeneous turbulent flow, the chance for a bubble to collide with an eddy that has sufficient energy to break the bubble is approximately [19]:

$$\eta_{ti} \propto \exp\left(-\frac{u_{t,cr}^2}{u_t^2}\right), \qquad (34)$$

where $u^2_{t,cr}$ is the critical mean square fluctuation velocity obtained from We_{cr}. Finally, for $\mathrm{We}>\mathrm{We}_{cr}$, the bubble breakup rate per unit mixture volume is given by:

$$R_{TI} = C_{TI}\exp\left(-\frac{\mathrm{We}_{cr}}{\mathrm{We}}\right)n\frac{u_t}{D}\left(1-\frac{\mathrm{We}_{cr}}{\mathrm{We}}\right)^{1/2}. \qquad (35)$$

Again, the adjustable parameters C_{TI} and We_{cr} should be evaluated with experimental data. This expression differs from the previous models [11, 12] because the breakup rate equals zero when the Weber number is less than We_{cr}. At low liquid flow rate with small void fraction, the turbulent fluctuation is small and thus no breakup would be counted. This unique feature was confirmed by experimental observations and allows the fine-tuning of the adjustable parameters in coalescence terms independently without considering the bubble breakage effect. Afterwards, the coefficients C_{TI} and We_{cr} may be found at relatively high liquid flow rate with fixed adjustable parameters in the coalescence terms.

III. ONE-GROUP INTERFACIAL AREA CONCENTRATION TRANSPORT EQUATION

In the two-fluid model, the parameter of interest is the interfacial area, a_i, rather than the bubble number density. To obtain the transport equation for interfacial area concentration, Eq. (2) can be modified with the following geometric relation:

$$n = \frac{\alpha}{\mathcal{V}_b} = \psi\left(\frac{a_i^3}{\alpha^2}\right) \tag{36}$$

where ψ is a factor depending on the shape of the bubbles. For spherical bubbles ψ equals $1/36\pi$. Substituting Eq. (36) into Eq. (2) leads to:

$$\frac{\partial a_i}{\partial t} + \nabla\cdot\left(a_i \overline{\overline{\mathbf{v}}}_g\right) = \frac{1}{3\psi}\left(\frac{\alpha}{a_i}\right)^2\left[\sum_j S_{n,j} + S_{n,ph}\right] + \left(\frac{2a}{3\alpha}\right)\left[\frac{\partial \alpha}{\partial t} + \nabla\cdot\left(\overline{\overline{\mathbf{v}}}_g \alpha\right)\right] \tag{37}$$

The second term on the right-hand-side represents the effects of void fraction variation. If the gas phase is assumed to be incompressible, without phase change the following continuity equation is applicable:

$$\frac{\partial \alpha}{\partial t} + \nabla\cdot\left(\alpha \overline{\overline{\mathbf{v}}}_g\right) = 0 . \tag{38}$$

Subsequently, the one-group interfacial area transport equation is reduced to:

$$\frac{\partial a_i}{\partial t} + \nabla\cdot\left(a_i \overline{\overline{\mathbf{v}}}_g\right) = \frac{1}{3\psi}\left(\frac{\alpha}{a_i}\right)^2 \sum_j S_{n,j} \tag{39}$$

With the models for the bubble number sink and source rates developed in section 2, the net rates of change in interfacial area concentration per unit mixture volume due to random collision, wake-entrainment and turbulent impact are given below, respectively.

Coalescence due to Random Collision:

$$S_{a,RC} = -\frac{C_{RC}\left(u_t a_i^2\right)}{3\pi\alpha_{\max}^{1/3}}\left[\frac{1}{\left(\alpha_{\max}^{1/3} - \alpha^{1/3}\right)}\right]\left[1 - \exp\left(-C\frac{\alpha_{\max}^{1/3}\alpha^{1/3}}{\alpha_{\max}^{1/3} - \alpha^{1/3}}\right)\right] \tag{40}$$

Coalescence due to Wake-Entrainment :

$$S_{a,WE} = -\frac{1}{3\pi} C_{WE} u_r a_i^2 . \tag{41}$$

Breakup due to Turbulent Impact:

$$S_{a,TI} = \frac{1}{18} C_{TI} u_t \left(\frac{a_i^2}{\alpha}\right)\left(1 - \frac{\mathrm{We}_{cr}}{\mathrm{We}}\right)^{1/2} \exp\left(-\frac{\mathrm{We}_{cr}}{\mathrm{We}}\right), \tag{42}$$

for $\mathrm{We} \geq \mathrm{We}_{cr}$.

Eqs. (39) to (42) constitute the one-group closure relation for interfacial area concentration in two-phase vertical dispersed bubbly flow. The variables in these equations are coupled with the field equations in the two-fluid model. For the information of the local interfacial area concentration, the field equations should be solved together with the closure relations. However, the presented model is limited only to the two-phase dispersed bubbly flow. At high void fraction when cap or slug bubbles appear, another transport equation should be provided for the interfacial area concentration of cap or slug bubbles. The two groups are not independent. The inter-group transfer terms should also be modeled individually. As shown in Fig. 1, these terms include the breakage of the cap bubbles with the daughter bubbles in the first group, the coalescence rate of the small bubbles with the daughter bubble in the second group, and the inter-group coalescence with the daughter bubble in the second group.

The study on the two-group transport equations for interfacial area concentration is the next phase task. However, if the present one-group model is justified with the existing experimental data, a solid foundation will be provided for the two-group approach. In such a way, the mechanisms as well as the source and sink terms presented in this paper can be isolated from the complicated fluid particle transfers between the two groups, and the evaluations to the presented models are more effective. To do so, the one-group model will be further reduced to a one-dimensional form in the next section by averaging over the cross-sectional area, and the model is then compared with experimental data obtained at different axial locations for vertical bubbly up-flows under steady state condition [18].

IV. EVALUATION OF THE ONE-GROUP MODEL

The simplest form of interfacial area transport equation is the one-dimensional formulation obtained by applying cross-sectional area averaging over Eq. (39):

$$\frac{\partial\langle a_i\rangle}{\partial t} + \frac{\partial}{\partial z}\left(\langle a_i\rangle\langle\langle \mathrm{v}_{gz}\rangle\rangle_a\right) = \langle S_{a,RC}\rangle + \langle S_{a,WE}\rangle + \langle S_{a,TI}\rangle \tag{43}$$

Due to the uniform bubble size assumption, the area-averaged bubble interface velocity weighted by interfacial area concentration can be given by:

$$\left\langle\left\langle v_{gz}\right\rangle\right\rangle_a \equiv \frac{\left\langle a_i v_{gz}\right\rangle}{\left\langle a_i\right\rangle} \approx \frac{\left\langle \alpha v_{gz}\right\rangle}{\left\langle \alpha\right\rangle}\left\langle\left\langle v_g\right\rangle\right\rangle, \qquad (44)$$

which is the same as the conventional area-averaged gas velocity weighted by void fraction, if the internal circulation in bubbles is neglected. The exact mathematical expressions for the area-averaged source and sink terms would involve many covariances that may further complicate the one-dimensional problem. However, since these local terms were originally obtained from a finite mixture element, the functional dependence of the area-averaged source and sink terms on the averaged parameters should be approximately the same if the hydraulic diameter of the flow path is considered the length scale of the finite element. Therefore, Eqs. (40), (41), and (42) with the parameters averaged within the cross-sectional area are still applicable for the area-averaged source and sink terms in Eq. (43).

To utilize the experimental data at different axial locations under steady-state condition, the transient term in Eq. (43) is dropped, leading to

$$\frac{d}{dz}\left(\left\langle a_i\right\rangle\left\langle\left\langle v_{gz}\right\rangle\right\rangle\right) = \left\langle S_{a,RC}\right\rangle + \left\langle S_{a,WE}\right\rangle + \left\langle S_{a,TI}\right\rangle. \quad (45)$$

Without phase change, the gas superficial velocity should be constant that is known from fixed flow conditions in the experiment, independent of the axial positions. Since the change of the gas velocity due to the mean bubble relative velocity variation is insignificant, the area-averaged void fraction is approximately constant. Thereafter, for a given flow condition, the only variable that should be specified is the energy dissipation rate per unit mixture mass, ε. A sophisticated approach is to couple the transport equation with the field equations and the constitutive relation of ε, such as the k-ε model (Bertodano, 1994 [27]). However, for the purpose of evaluating the model in one-dimensional form, the following simple algebraic correlation for ε is employed in this study without solving the momentum equation:

$$\varepsilon = f_{TW}\frac{1}{2D_h}\left\langle v_m\right\rangle^3, \qquad (46)$$

where, $\left\langle v_m\right\rangle$ denotes the mean mixture velocity, D_h refers to the hydraulic diameter of the flow path, and f_{TW} is the two-phase friction factor (Todreas, 1989 [36]):

$$f_{TW} = f_f\left(\frac{\mu_m}{\mu_f}\right)^{0.25} = \frac{0.316}{\mathrm{Re}_m^{0.25}}\left(\frac{\mu_m}{\mu_f}\right)^{0.25}. \qquad (47)$$

For dispersed bubbly flow, the mixture viscosity, μ_m, is given by (Ishii and Chawla, 1979 [34]):

$$\mu_m = \frac{\mu_f}{\left(1-\left\langle\alpha\right\rangle\right)} \qquad (48)$$

To identify the adjustable parameters in the source and sink terms, experimental data of a steady air-water concurrent up-flow in a 5.08 cm pipe (Kashyap et al, 1994 [18]) are used. In their experiments, interfacial area concentration and void fraction were measured with a double-sensor conductivity probe at three different axial positions (L/D_h=2, 32, 62). In Table 1, seven cases of tests are summarized for different flow conditions. With the measured interfacial area concentration at L/D_h=2 as the initial condition, Eq. (45) is integrated numerically to predict the axial distribution of interfacial area concentration. The process involves the algebraic correlation of the energy dissipation rate per unit mixture mass specified in Eq. (46), in order to decouple the momentum equations from the interfacial area transport equation and the continuity equations. Subsequently, the adjustable parameters in the models are determined if the predictions at the other two locations match the experimental data.

Table 1 Test conditions (Kashyap et al.)

	$\langle j_g\rangle$ (m/s)	$\langle j_f\rangle$ (m/s)	$\langle\alpha\rangle$
case 1	0.023	0.77	~2.5%
case 2	0.117	0.77	~10.0%
case 3	0.058	1.11	~4.0%
case 4	0.117	1.11	~7.0%
case 5	0.023	1.58	~1.6%
case 6	0.058	1.58	~3.0%
case 7	0.117	1.58	~6.5%

Table 2 Adjustable parameters

C_{RC}	C	C_{WE}	C_{TI}	We_{cr}
0.0565	3	0.151	0.18	2.0

At low liquid flow rate with small void fraction, bubble breakage can be neglected due to the very small Weber number compared to the critical value. In such a case, the fitting involves only 3 constants, i.e. C_{RC}, C, and C_{WE}. In fact, only two sets of data were employed in the process. After these parameters are fixed, the

transport equation is further applied to one high flow rate condition solely for C_{TI} and We_{cr}. The final results of these adjustable parameters are summarized in Table 2. For the wake entrainment mechanism, the coefficient is 0.122. Assuming a flat cross-sectional wake velocity profile, the effective wake length for bubble coalescence estimated from Eqs. (26) and (27) is about 7 times the mean bubble diameter, which agrees with the observation of Tsuchiya et al. (1989 [33]). For bubble breakup, the critical Weber number is found to be 2.0 for the best fit to the experimental data, which is slightly smaller than 2.3, a value suggested by Prince and Blanch (1990 [11]). This discrepancy may be caused by the one-group approach assuming uniform bubble size. In reality, bubble breakage exists as long as the size of certain bubbles reaches the breakup limit in spite of the fact that the mean size does not exceed it. Therefore, the critical Weber number for bubble breakage based on the average bubble size should be smaller than that based on the actual size of a breaking bubble.

At a very low liquid flow rate with a small void fraction as in the case 1, no bubble breakage is expected. Fig. 5 illustrates such a variation in the area-averaged interfacial area concentration along the flow path. No bubble breakage is involved because the Weber number is smaller than the critical value. Since the void fraction is small, the drop of the interfacial area concentration caused by random collisions is only about one tenth of total decrease. However, as the void fraction increases to 10% in case 2 with the same liquid superficial velocity as in case 1, the change in interfacial area concentration due to random collisions increases to roughly 20% of the total change as shown in Fig. 6. Moreover, because of the large coalescence rate, the mean bubble size grows rapidly. At about L/D_h=40, the bubble Weber number becomes greater than the critical value and thus the bubble breakage term takes effect, resulting in a slower overall decrease in interfacial area concentration along the flow path.

An extreme condition is for case 7 as shown in Fig. 7 with a liquid superficial velocity of 1.58 m/s, and bubble breakage exists at the very beginning. In this case, the coalescence rate seems to be balanced by the breakup rate along the flow path, resulting in a relatively flat axial distribution of the interfacial area concentration.

By applying these adjustable coefficients obtained from only three sets of experimental data to the other flow conditions, the results are presented in Figs. 8a and 8b. The model predictions of the changes in interfacial area concentrations are generally in good agreement with the measurements. The maximum relative difference is

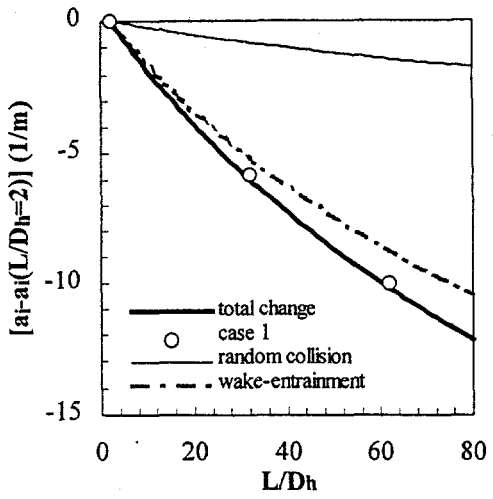

Fig. 5 Axial variation of $<a_i>$ for case 1

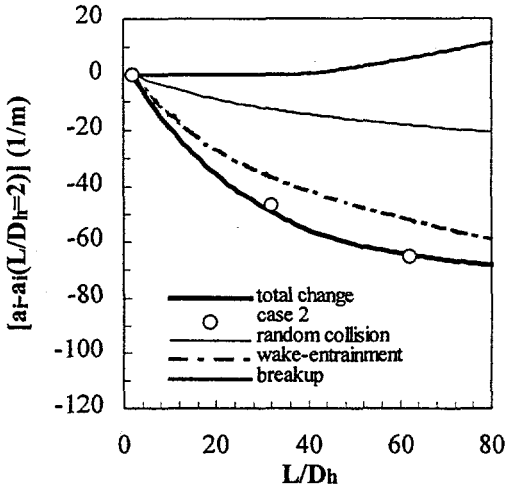

Fig. 6 Axial variation of $<a_i>$ for case 2.

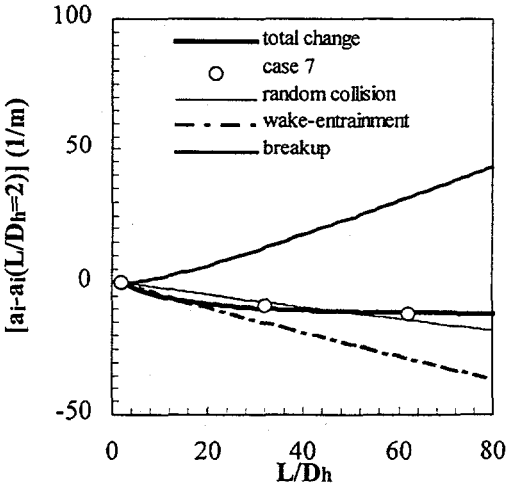

Fig. 7 Axial variation of $<a_i>$ for case 7.

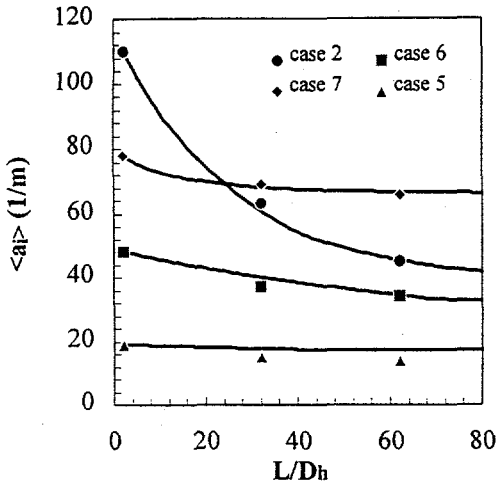

Fig. 8a Axial variation of $<a_i>$ for case 2, 5, 6, and 7

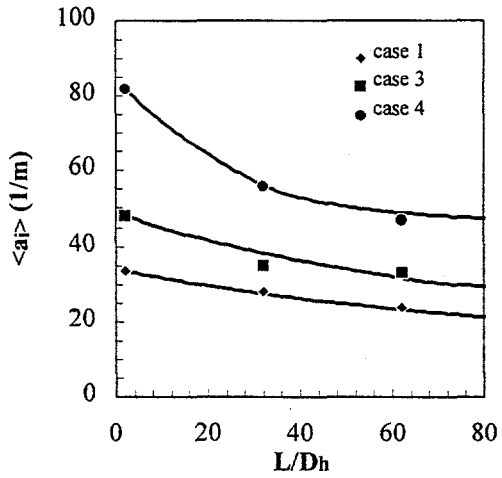

Fig. 8b Axial variation of $<a_i>$ for case 1, 3, and 4

about 8% at a very small void fraction with high liquid flow rate. Nevertheless, the conclusion is based on the only set of the published experimental data that have three axial measurements for each flow condition. Fine-tuning of these adjustable parameters is needed when more data become available.

V. CONCLUSIONS

In this study, a one-group interfacial area transport equation together with the modeling of the source and sink terms for bubble breakup and coalescence was presented. For bubble coalescence, two mechanisms were considered to be dominant in vertical two-phase bubbly flow. These include the random collisions between bubbles due to turbulence in the flow field, and the wake entrainment process due to the relative motion of the bubbles in the wake region of a seeding bubble. For bubble breakup, the impact of turbulent eddies was included. These phenomena were modeled individually, resulting in a one-group interfacial area concentration transport equation with certain parameters to be determined from experimental data.

By area-averaging over the local one-group transport equation, a one-dimensional form of interfacial area concentration transport equation was obtained. Compared to experimental data for the axial distribution of the interfacial area concentration under various flow conditions, the adjustable parameters in the model were obtained. The results indicate that the proposed models for bubble breakup and coalescence are appropriate. The ranges of the adjustable parameters agree with the physical observations. However, the comparison was based on the only set of published experimental data that have three axial measurements for each flow condition. Fine-tuning of these adjustable parameters is needed when more data become available, especially for three-dimensional analysis. The adjustable parameters for application of the localized transport equation have to be verified through the coupling to the three-dimensional two-fluid model with a k-ε model added.

AKNOWLEDGEMENTS

This study was supported by Westinghouse Bettis Atomic Power Laboratory. The authors would like to express their gratitude to the reviewers for their valuable suggestions and comments.

NOMENCLATURE

English

a_i	interfacial area concentration
C	constants
C_D	bubble drag coefficient
D	bubble Sauter mean diameter
D_h	hydraulic diameter
f_{tw}	two-phase friction factor
j	superficial velocity
L	length
L_w	bubble wake length
n	bubble number density
r	collision frequency for two bubbles
R	collision rate
Re	Reynolds number
s	volume dependent source/sink terms
S	source/sink terms
t	time
u_r	relative velocity

u_t	RMS fluctuating velocity
v	velocity
$\mathscr{V}$	bubble volume
We	Weber number
x	space coordinates
z	flow direction coordinate
ΔT	time interval

Greek Symbols

α	void fraction
δ	parameter defined in text
ε	averaging factor
γ	parameter defined in text
η	coalescence efficiency
μ	dynamic viscosity
ρ	density
σ	surface tension

Subscript

a	interfacial area concentration
b	bubble
cr	critical
D	bubble
e	effective
f	liquid
g	gas
h	hydraulic
i	interfacial
j	index of summation
m	mixture
max	maximum
n	bubble number density
p	particle/bubble
ph	phase change
pm	bubble mean value
RC	random collision
t	turbulent
TI	turbulent impact
$\mathscr{V}$	bubble volume
w	bubble wake
WE	wake entrainment
z	flow direction

REFERENCES

1. P. Vernier and J.M. Delhaye, "General two-phase flow equations applied to the thermohydrodynamics of boiling nuclear reactor," Engr. Primaire, Vol. No. 1, 5 (1968).
2. G. Kocamustafaogullari, "Thermofluid dynamics of separated two-phase flow," Ph.D. Thesis, Georgia Institute of Technology (1971).
3. M. Ishii, *Thermo-Fluid Dynamic Theory of Two-Phase Flow*, Collection de la Drection des Etudes et Reserches d'Electricité de France, Eyrolles, Paris (1975).
4. J.A. Boure, "Mathematical modeling of two-phase flows," Proc. of CSNI Specialist Meeting, S. Banerjee and K.R. Weaver, Eds. A.E.C.L., Vol. 1, 85, Aug. 3-4, Toronto (1978).
5. M. Ishii and K. Mishima, "Study of Two-fluid Model and Interfacial Area," Argonne National Laboratory Report, ANL-80-111 (1980).
6. J.N. Reyes, "Statistically derived conservation equations for fluid particle flows," 5th Proc. ANS-THD, P. 12, 1989 ANS Winter Meeting, San Francisco, CA, Nov. (1989).
7. F.A. Williams, *Combustion Theory*, Addison-Wesley Publishing Co., Reading, Mass. (1965).
8. G. Kocamustafaogullari and M. Ishii, "Foundation of the interfacial area transport equation and its closure relation," *Int. J. Heat and Mass Transfer*, Vol. 38, No. 3, 481 (1995).
9. A.A. Shraiber, "Comments on 'Foundation of the interfacial area transport equation and its closure relations'", *Int. J. of Heat and Mass Transfer*, Vol. 39, No. 5, 1117 (1996).
10. G. Kocamustafaogullari and M. Ishii, "Interfacial area and nucleation site density in boiling systems," *Int. J. Heat and Mass Transfer*, Vol. 26, 1377 (1983).
11. M.J. Prince and H.W. Blanch, "Bubble coalescence and break-up in air-sparged bubble columns," AIChE Journal, Vol. 36, No. 10, 1485 (1990).
12. A.Y. Lafi and J.N. Reyes, Jr., "Phenomenological Models for Fluid Particle Coalescence and Breakage," OSU-NE-9120, Report of the Department of Nuclear Engineering, Oregon State University, Corvallis, Oregon 97331, USA (1991).
13. M. Ishii and G. Kojasoy, "Interfacial area transport equation and preliminary considerations," PU-NE-93/6, Report of the Nuclear Engineering Department, Purdue University, West Lafayette, IN 47907, USA (1993).
14. S.K. Friedlander, *Smoke, Dust and Haze*, Wiley, New York (1977).
15. G.I. Taylor, "The formation of emulsion in definable field of flow," Proc. R. Soc., (London) Series, Vol. A146, 501 (1934).

16. D.A. Drew and R.T. Lahey Jr., "The virtual mass and lift force on a sphere in rotating and straining inviscid flow," *Int. J. Multiphase Flow*, Vol. 13, No. 1, 113 (1987).

17. R. Clift, J.R. Grace and M.E. Weber, *Bubbles, Drops, and Particles*, Academic Press, Inc., New York (1978).

18. A. Kashyap, M. Ishii and S.T. Revankar, "An experimental and numerical analysis of structural development of two-phase flow," PU-NE-94/2, Report of the Nuclear Engineering Department, Purdue University, West Lafayette, IN 47907, USA (1994).

19. C.A. Coulaloglu and L.L. Tavlarrides, "Drop size distributions and coalescence frequencies of liquid-liquid dispersion in flow vessels," *AIChE J.*, Vol. 22, 289 (1976).

20. T. Oolman and H.W. Blanch, "Bubble coalescence in stagnant liquids," *Chem. Eng. Commun.*, Vol. 43, 237 (1986).

21. R.D. Kirkpatrick and M.J. Lockett, "The influence of approach velocity on bubble coalescence," *Chem. Eng. Sci.*, Vol. 29, 2363 (1974).

22. G.B. Wallis, *One-dimensional Two-phase Flow*, McGraw-Hill Book Company, NY. 350 (1969).

23. G.K. Batchelor, "Pressure fluctuation in isotropic turbulence," *Proc. Cambridge Phil. Soc.*, Vol. 47, 359 (1951).

24. S.J. Lee, R.T. Lahey, Jr., and O.C. Jones, "The prediction of two-phase turbulence and phase distribution using k-e model," Ph.D. Thesis, Department of Nuclear Engineering, Rensselaer Polytechnic Institute, Troy, NY (1986).

25. I. Kataoka and A. Serizawa, "Turbulent suppression in bubbly two-phase flow," *J. of Nuclear Engineering and Design*, Vol. 122, 1 (1991).

26. M. Lopez de Bertodano, R.T. Lahey, Jr., and O.C. Jones, "Development of a k-ε model for bubbly to-phase flow," *J. of Fluids Engineering*, Vol. 116, 128 (1994).

27. Noel de Nevers and J.L. Wu, "Bubble coalescence in viscous fluids," *AIChE Journal*, Vol. 17, No. 1, 182 (1971).

28. T. Otake, S. Tone, K. Nakao, and Y. Mitsubashi, "Coalescence and breakup of bubbles in liquids," *Chem. Eng. Sci.*, Vol. 32, 377 (1977).

29. Z. Bilicki and J. Kestin, "Transition criteria for two-phase flow patterns in vertical upward flow," *Int. J. Multiphase Flow*, Vol. 13, No. 3, 283 (1987).

30. C.W. Stewart, "Bubble interaction in low-viscosity liquid," *Int. J. Multiphase Flow*, Vol. 21, No. 6, 1037 (1995).

31. J. Katz and C. Meneveau, "Wake-induced relative motion of bubbles rising in line," *Int. J. Multiphase Flow*, Vol. 22, No. 2, 239 (1996).

32. F.M. White, *Viscous Fluid Flow*, 2nd edition, McGraw-Hill, Inc., NY, p. 481 (1991).

33. K. Tsuchiya, T. Miyahara, and L.S. Fan, "Visualization of bubble-wake interactions for a stream of bubble in a two-dimensional liquid solid fluidized bed," *Int. J. Multiphase Flow*, Vol. 15, No. 1, 35 (1989).

34. M. Ishii and T.C. Chawla, "Local drag laws in dispersed two-phase flow," NUREG/CR-1230, ANL-79-105 (1979).

35. M. Sevik and S.H. Park, "The splitting of drops and bubbles by turbulent fluid flow," *J. Fluids Eng.*, Vol. 3, 53 (1973).

36. N.E. Todreas and M.S. Kazimi, *Nuclear System I: Thermal Hydraulics Fundamentals*, Taylor & Francis, Bristol, PA, 489 (1989).